

Mild Chronic Colitis Exacerbates Intracerebral Inflammation in Mice with Parkinson's Disease Through LRRK2-Mediated Regulation of NF- κ B Activation and Inhibition of Nrf2

Manqi Yang^{1,*}, Linping Ke^{1,*}, Yiman Geng¹, Piao Hu¹, Yao Qiu¹, Ziwen Liu¹, Xueqin Zhang¹, Fuxin Wan¹, Joe Antony Jacob², Jingling Liao¹

¹Academy of Nutrition and Health, Hubei Province Key Laboratory of Occupational Hazard Identification and Control, School of Public Health, Wuhan University of Science and Technology, Wuhan, 430065, People's Republic of China; ²Department of Biomaterials, Saveetha Dental College and Hospitals, Saveetha Institute of Medical and Technical Sciences (SIMATS), Saveetha University, Chennai, Tamil Nadu, 600077, India

*These authors contributed equally to this work

Correspondence: Jingling Liao, Academy of Nutrition and Health, Hubei Province Key Laboratory of Occupational Hazard Identification and Control, School of Public Health, Wuhan University of Science and Technology, Wuhan, 430065, People's Republic of China, Email jinglingliao@wust.edu.cn

Background and Objective: Inflammatory bowel disease (IBD) is a known risk factor for Parkinson's disease (PD). Leucine-rich repeat kinase 2 (LRRK2), a protein associated with both disease, regulates inflammation in the colon and brain. However, the precise mechanism by which LRRK2 mediates the crosstalk between intestinal inflammation and PD neuropathology remains unclear. This study aims to elucidate how LRRK2 mediates the inflammatory response in both the gut and brain.

Methods: A dual-hit (DSS+MPTP) mouse model was established to induce IBD and PD, along with separate single DSS-induced colitis and MPTP-induced PD models. LRRK2 expression was analyzed in the colon and striatum. Intestinal barrier integrity (ZO-1, Occludin), dopaminergic neuron loss and inflammation (TH, Iba-1 staining in SNpc/striatum), NF- κ B and Nrf2 pathways activity, and levels of inflammatory cytokines (TNF- α , IL1- β , IL-6 and IL-10) in the colon and striatum was assessed.

Results: In the colon, LRRK2 expression was significantly increased in all experimental groups compared to the control, with the highest levels observed in the dual-hit group. The elevated LRRK2 expression correlated with the reduction in ZO-1 and Occludin levels and an increase in inflammatory cytokines IL1- β and TNF- α . A similar pattern of LRRK2 expression was observed in the brain. The dual-hit group exhibited increased Iba-1 expression and a significant loss of dopaminergic neurons. Furthermore, the upregulation of LRRK2 was associated with NF- κ B activation and Nrf2 inhibition in the brain.

Conclusion: Mild chronic colitis induced by DSS may exacerbate brain inflammation in MPTP-induced PD mice by upregulating LRRK2 expression, leading to NF- κ B activation and Nrf2 inhibition. We propose that LRRK2 may play a regulatory role in the NF- κ B/Nrf2 interplay in PD.

Keywords: parkinson's disease, inflammatory bowel disease, LRRK2, inflammation, NF- κ B, Nrf2/HO-1

Introduction

Parkinson's disease (PD) is an irreversible neurodegenerative disorder projected to affect over 14 million people by 2040, with no effective treatment available.¹ Neuron loss due to cell-autonomous death is widely regarded as the primary cause of PD.² Recent evidence has demonstrated that factors outside the central nervous system (CNS), particularly the immune-inflammatory response, also play a significant role. For instance, T-cell infiltration, especially in the substantia nigra, can be observed in the brain tissue of patients with PD and an MPTP mouse model.³ Additionally, the presence of Th17 cells, which drive inflammation, has been linked to the degeneration of dopaminergic cells and stem cells in PD via IL-17.⁴ In addition, Wang et al reported that inflammation plays an aggregating role in PD patients carrying wild-type α -syn.⁵ Indeed,

most individuals diagnosed with PD also experience gastrointestinal (GI) dysfunction, including constipation and vomiting.^{6,7} Inflammatory bowel disease (IBD), which encompasses Crohn's disease (CD) and ulcerative colitis (UC), is a chronic condition. Epidemiological studies have shown that patients with IBD are at higher risk for developing PD, supporting the hypothesis that intestinal disease may be a risk factor for PD.⁸ Additionally, treatment with anti-TNF- α in IBD patients has been found to reduce the risk of development of PD, further emphasizing the role of enterocolitis in PD pathogenesis.⁹

However, most previous studies have primarily focused on changes in the gut microbiota.^{10,11} IBD patients exhibit a reduction in anti-inflammatory bacteria and an increase in lipopolysaccharide (LPS)-producing bacteria within their gut microbiome. These microbiota disturbances can increase intestinal permeability, allowing metabolites to enter the circulatory system and trigger neuroinflammation via the gut-brain axis. Moreover, IBD-associated dysbiosis can disrupt neurotransmitter homeostasis through vagal pathways, short-chain fatty acid, and other mechanisms, which may cause non-motor PD symptoms to appear before the motor symptoms.^{12,13} Supporting this claim, certain studies have concluded that the gut-derived pro-inflammatory environment exacerbated the PD phenotype through a dysfunctional microbiota-gut-brain axis.^{14,15} However, the molecular inflammatory mechanisms through which IBD modulates PD remain underexplored.

In the context of PD, the leucine-rich repeat kinase 2 (LRRK2) gene has been identified as a significant contributor to its development.¹⁶ Genome-wide association studies have demonstrated a correlation between LRRK2 variants and the risk of inflammatory bowel disease (IBD); notably, variants such as G2019S and N2018D are linked to an increased risk of developing both PD and Crohn's disease (CD).¹⁷ Accumulating evidence suggests that inflammation may be a key mechanism by which LRRK2 influences the pathogenesis of both PD and IBD.^{17,18} Notably, LRRK2 is highly expressed in immune cells, including monocytes, neutrophils, and dendritic cells. Studies indicate that LRRK2 and its variants can induce microglia hyperactivation, trigger immune-inflammatory response, and regulate the activation of NLRP3 inflammasomes, all of which may contribute to Parkinson's disease progression.¹⁹ For instance, one study using LRRK2 R1441G knock-in mice found that microglia activated by LPS exhibited increased levels of pro-inflammatory factors and decreased levels of anti-inflammatory factors.²⁰ Moreover, in an animal model of PD, increased LRRK2 expression was associated with elevated levels of CD68 and iNOS in microglia, accompanied by the secretion of pro-inflammatory cytokines such as IL-10 and TNF- α , thereby accelerating dopaminergic neuronal loss.²¹ In a mouse model of experimental colitis induced by dextran sulfate sodium (DSS), DSS treatment was shown to increase interferon- γ (IFN- γ) expression and LRRK2 phosphorylation in the colon tissue, suggesting an interaction between IFN- γ and LRRK2 in the gut under inflammatory conditions.²² Furthermore, LRRK2-deficient mice exhibited greater susceptibility to DSS-induced colitis.²³ These findings imply that LRRK2 may negatively modulate the inflammatory response during colitis. In addition, mice carrying the LRRK2 G2019S mutation showed a significant increase in α -synuclein aggregation and dopaminergic neuronal loss in the substantia nigra following chronic intestinal inflammation, with these effects being more pronounced in male mice. LRRK2 appears to exacerbate PD-related neuroinflammation by promoting the release of inflammatory factors via activation of the NF- κ B pathway.²⁴ Moreover, metabolites from the gut flora of IBD patients activate LRRK2 through TLR4, which stimulates NF- κ B signaling and establishes a pro-inflammatory feedback loop. Inhibitors of LRRK2 kinase activity have been shown to alleviate inflammatory symptoms in colitis models.²⁵ Additionally, Chi et al reported that LRRK2 deficiency results in paradoxical responses and reduces IFN signaling in microglia, indicating that Nrf2 is regulated by LRRK2 activity.²⁶ Collectively, these findings underscore the critical regulatory role of LRRK2 in inflammatory responses in both the colon and the brain. However, whether LRRK2 enhances the inflammatory responses in a dual-hit animal model induced by DSS and MPTP—its precise role in the crosstalk between intestinal inflammation and PD neuropathology—remains to be fully elucidated.

To address the questions, we established three mouse models. First, a PD model was constructed by intraperitoneal injection of 1-methyl-4-phenyl-1,2,3,6-tetrahydropyridine (MPTP). Second, an intestinal inflammation model was generated by free drinking water containing DSS. Third, a dual-hit model was induced by treating mice with DSS followed by MPTP injection. We then examined the expression levels of LRRK2 and inflammatory molecules (TNF- α , IL1- β , IL-6, etc.) in both the brains and intestines of these models. Our results demonstrated that DSS-induced colitis may trigger an inflammatory response in the brain by upregulating LRRK2 expression levels, which may in turn exacerbate the inflammatory response in PD mice.

Materials and Methods

Animals

Forty-five male C57BL/6 mice, approximately 8 weeks and weighing about 25 ± 5 g, were purchased from Jiangsu Huachuang Xinnuo Pharmaceutical Science and Technology Co(SCXK(Jiangsu)2020-0009). After arrival, the mice were acclimatized for one week in SPF environment, during which they had free access to food and water. They were housed in a controlled environment with a temperature of 25°C , relative humidity of 50–60% and a 12-h light/dark cycle. Throughout the procedures, anesthesia was administered to minimize the pain for the mice. All animal experimental procedures were conducted in accordance with the guidelines for Ethical Review of Experimental Animal Welfare (GB/T35892-2018) issued by China and received approval from Wuhan University of Science and Technology (Ethical approval number WUST2025019).

MPTP and DSS Treatment

Parkinson's disease was induced in mice by intraperitoneal injection of MPTP (M9208090, Yeasen Biotechnology) for one consecutive week.²⁷ Ulcerative colitis was induced by allowing the animals to consume drinking water containing DSS (D2230081, Yeasen Biotechnology) *ad libitum*. The animals were randomly divided into four groups: Control ($n=10$), which consisted of animals drinking tap water and receiving saline injections; MPTP ($n=10$), which included animals receiving MPTP injections at a dose of 30mg/kg once per day for one week; DSS ($n=10$), which comprised animals drinking a water containing 3% DSS for three weeks (this consisted of four consecutive days of drinking DSS-containing water followed by three days of cessation, repeated for three weeks); and MPTP+DSS ($n=15$), which included animals drinking a water containing 3% DSS and receiving MPTP injections at reduced dose of 15mg/kg once per day. The dose of MPTP was halved in this group due to concerns regarding mortality based on findings from previous studies.^{28,29} At the end of the behavioral assessment period, the mice were sacrificed, and their brains, spleens, and colons were collected for further analysis.

H&E Staining and Histological Scoring of the Colon

After euthanasia, the colon was cut out and washed with ice-cold PBS. The distal third section of the colon was then placed in 4% paraformaldehyde overnight for fixation. The tissue was subsequently embedded in paraffin, sectioned and stained with hematoxylin-eosin (H&E). The colon sections were first deparaffinized in xylene and then rehydrated in graded ethanol of 100% and 75%. Following rehydration, hematoxylin stain was applied for 3–5 minutes. After that, the sections were subjected to dehydration using 85% and 95% graded ethanol, and then the sections were stained with eosin for 5 minutes. Finally, the sections were dehydrated again and mounted with neutral gum.

The histological colitis score was determined based on published literature.³⁰ H&E colon stained sections from different experimental groups were scored using a five-point grading scale: (i) Epithelial cells in a normal pattern without inflammatory infiltration, score 0; (ii) loss of goblet cells and inflammatory infiltration around the base of the crypts, score 1; (iii) extensive loss of cup cells and inflammatory infiltration reaching the mucosal musculature, score 2; (iv) Loss of crypts with extensive infiltration of inflammation into the mucosal musculature, accompanied by mucosal thickening and extensive oedema, score 3; (v) extensive loss of crypts with inflammatory infiltration reaching the submucosal layer, score 4. Scores were assessed separately by two graders in a single-blind way.

Disease Activity Index (DAI)

The DAI is an important measure for assessing colitis, and it is evaluated through three main criteria: body weight loss, fecal consistency, and the presence of blood in the stool. The DAI score is categorized into the following 5 levels: (i) Score 0: weight loss $<1\%$, normal stool consistency, no occult blood; (ii) Score 1: weight loss 1%–5%, weakly positive for occult blood, stool consistency remains normal; (iii) Score 2: weight loss 5%–10%, loose stools, half-formed, positive for occult blood; (iv) Score 3: weight loss 10%–15%, strongly positive for occult blood, stool consistency is significant altered; (v) Score 4: weight loss $>15\%$, watery stools, shapeless, and visible blood in stool.³¹ The total DAI scores range from 0 to 16.

Behavioral Assays

Rotarod Test

As part of the pre-training trials, mice were placed on a rotarod set at 4 rpm for 5 min on two consecutive days. Following this, the instrument parameters were adjusted to a baseline speed of 4 rpm for 5 seconds, followed by a gradual acceleration from 4 to 60 rpm over a 10-minute period. The instrument automatically detected the drop of the mice, and the time each mouse spent on the rotarod was recorded as the latency to fall. Final result was obtained by conducting three trials at intervals of 30 min.

Open Field Test (OFT)

The animals were placed in a white cube box measuring 50×50×40 cm (Shanghai XinRuan Information Technology Co. Ltd., XR-XZ301). A glass beaker was positioned in the center of the bottom of the box, and the mice were recorded on video while they were allowed to explore freely for 5 minutes. The experiment was performed in a quiet environment. All activities were automatically recorded by the apparatus, and indicators such as total movement distance, distance from the center area, and time spent in the center area were analyzed to evaluate the animal's anxiety level.

Nissl Staining

After euthanasia, the brains were separated and washed with ice-cold PBS. The brains were then placed in 4% paraformaldehyde overnight for fixation. The tissue was subsequently embedded in paraffin and sectioned. The striatum and SNpc sections were deparaffinized as previously described and then incubated in Nystad stain (G1036, Servicebio) for 2 to 5 minutes. Differentiation was achieved using 0.1% glacial acetic acid, and the sections were washed in tap water to halt the reaction. The degree of differentiation was assessed under a microscope. Afterwards, the sections were placed in clear xylene for 10 minutes and subsequently sealed with neutral gum.

Immunohistochemistry

The brain and colon tissue sections were deparaffinized and configured with sodium citrate solution for microwave hyperthermia to repair antigens. They were permeabilized with PBS containing 0.2% Triton X-100 for 10 minutes and incubated with 3% H₂O₂ to reduce endogenous peroxidase activity. Next, the sections were blocked with 10% goat serum for 30 minutes at room temperature, followed by overnight incubation at 4°C with primary antibodies: rabbit anti-TH antibody (1:500; 58844S, CST), rabbit anti-Iba1 antibody (1:800; 17198S, CST), rabbit anti-ZO-1 antibody (1:125; AF5145, Affinity), rabbit anti-Occludin antibody (1:125; DF7504, Affinity). The following day, sections were removed, allowed to equilibrate to room temperature, and then incubated with IgG (PV-6000, ORIGENE) for 30 minutes. Color development was achieved using a DAB kit (G1212, Servicebio), followed by nuclei staining with hematoxylin (KR0125, Wuhan Kerui Biotechnology Co., LTD). and differentiation with 1% hydrochloric acid alcohol. Images were captured using a full-wavelength scanner (VS200, Olympus). Optical density values were analyzed using Image J 1.52p software (NIH, USA).

Western Blotting

The colon and striatum samples were added to RIPA lysis buffer containing protease and phosphatase inhibitors (78442, Thermo). The total protein concentration in the supernatant was determined by the BCA method (KR0008, Wuhan Kerui Biotechnology Co., LTD). After mixing the supernatant with 1× loading buffer and denaturing it at 95°C, proteins were transferred to PVDF membranes following thorough SDS-polyacrylamide gel electrophoresis. The PVDF membranes were blocked with 5% milk or 5% BSA for 1 hour at room temperature, then incubated with primary antibody overnight at 4°C. On the following day, the membranes were incubated with secondary antibody for 1 hour at room temperature. Blots were visualized using the imaging system, and the relative levels of protein expression were quantified using Image J software. The following antibodies were primarily used in this experiment: rabbit anti-LRRK2 antibody (1:5000; 5559S, CST), rabbit anti-HO-1 antibody (1:1000; WL02400, Wanleibio), rabbit anti-Nrf2 antibody (1:5000; 80,593-1-RR, Proteintech), rabbit anti-NF-κB p65 antibody (1:5000; 80,979-1-RR, Proteintech), rabbit anti-phospho-NF-κB p65 antibody (Ser536) (1:5000; AF2006, Affinity Biosciences), rabbit anti-IL-6 antibody (1:1000; DF6087, Affinity Biosciences), rabbit anti-IL-10 antibody (1:1000; WL03088, Wanleibio), rabbit anti-Iba1 antibody (1:1000; 17198S, CST), mouse anti-GAPDH antibody (1:10,000; 6004-1-Ig, Proteintech).

RNA Isolation and RT-qPCR Analysis

Striatum and colon samples were weighed, and RNA was extracted using an isolation kit (1071073, QIAGEN). The purity and concentration of the extracted RNA was determined using a NanoDrop spectrophotometer (Thermo Fisher Science, Inc). RNA was then reverse transcribed into cDNA using a reverse transcription kit containing gDNA Eraser (RR047A, TAKARA). The relative mRNA expression levels of various genes in the samples were detected by quantitative real-time polymerase reaction (qPCR) using the SYBR-Green method (CFX384, BIO-RAD). The relative expression of each gene was calculated using the $2^{-\Delta\Delta C_t}$ method, with the expression of glyceraldehyde-3-phosphate dehydrogenase (GAPDH) serving as a standardized control. The primers used in this study are listed in Table 1.

Statistical Analysis

Statistical analysis was performed using GraphPad Prism 10 software. Multiple comparisons between groups were analyzed using two-way ANOVA, followed by LSD multiple comparison tests. Data were expressed as mean \pm SEM, and differences were considered statistically significant at $p < 0.05$.

Results

Characterization and Behavior Assays in Animal Models

Many studies have demonstrated the critical regulatory role of LRRK2 in inflammatory responses in both the colon and the brain. To investigate whether LRRK2 enhances exacerbates inflammatory responses in the brain when colitis and PD co-exist, we established three mouse models in the present study. First, a PD model was constructed by intraperitoneal injection of MPTP (MPTP group). Second, an intestinal inflammation model was generated by free drinking water containing DSS (DSS group). Third, a dual-hit model was induced by treating mice with DSS followed by MPTP injection (DSS+MPTP group) (Figure 1A). We weighed the mice daily and observed the significant decreases in body weight ($p < 0.01$) in the DSS and DSS+MPTP groups compared to the control group, which only drank tap water (Figure 1B). To assess the severity of the colitis, DAI scores were recorded. Based on the comparison of DAI scores among the groups, the control and MPTP groups exhibited normal scores, whereas the DSS and DSS+MPTP groups showed significant severity ($p < 0.0001$). Moreover, the severity of DSS+MPTP group was greater than that of the DSS group ($p < 0.05$) (Figure 1C). This interesting result suggests that the MPTP-induced alterations in the brain may aggravate colitis in mice.

Spleen weight is a key indicator of the severity of inflammation, as splenomegaly reflects heightened production and release of immune cells.³² A significant increase in spleen weight was observed in the MPTP ($p < 0.01$) and DSS ($p < 0.05$) groups compared to the control group. However, the DSS+MPTP group did not show a significant increase in spleen weight, although a tendency towards increased spleen weight was observed; its spleen weight was significantly lower than that of the MPTP group ($p < 0.05$) (Figure 1D–E). These results imply that both colitis and PD may provoke a systemic inflammatory response.

Table 1 qPCR Primers Used in the Study

Gene Name	Primer Sequence (5'→3')
GAPDH	Forward-5'-AGGAGCGAGACCCCACTAACA-3' Reverse-5'-AGGGGGGCTAAGCAGTTGGT-3'
LRRK2	Forward-5'-TGCCATGCACAGATATTCAGC-3' Reverse-5'-TGCAAGCAGCAAAGTACGTG-3'
IL-1 β	Forward-5'-CACAGCAGCACATCAACAAG-3' Reverse-5'-GTGCTCATGTCCTCATCCTG-3'
TNF- α	Forward-5'-ATGAGAAGTCCCAAATGGC-3' Reverse-5'-CTCCACTTGGTGGTTTGCTA-3'
IL-6	Forward-5'-AAAATCATTAACTCCCTGTTGAT-3' Reverse-5'-TAAGCCTCCGACTTGTGAAGTGGT-3'

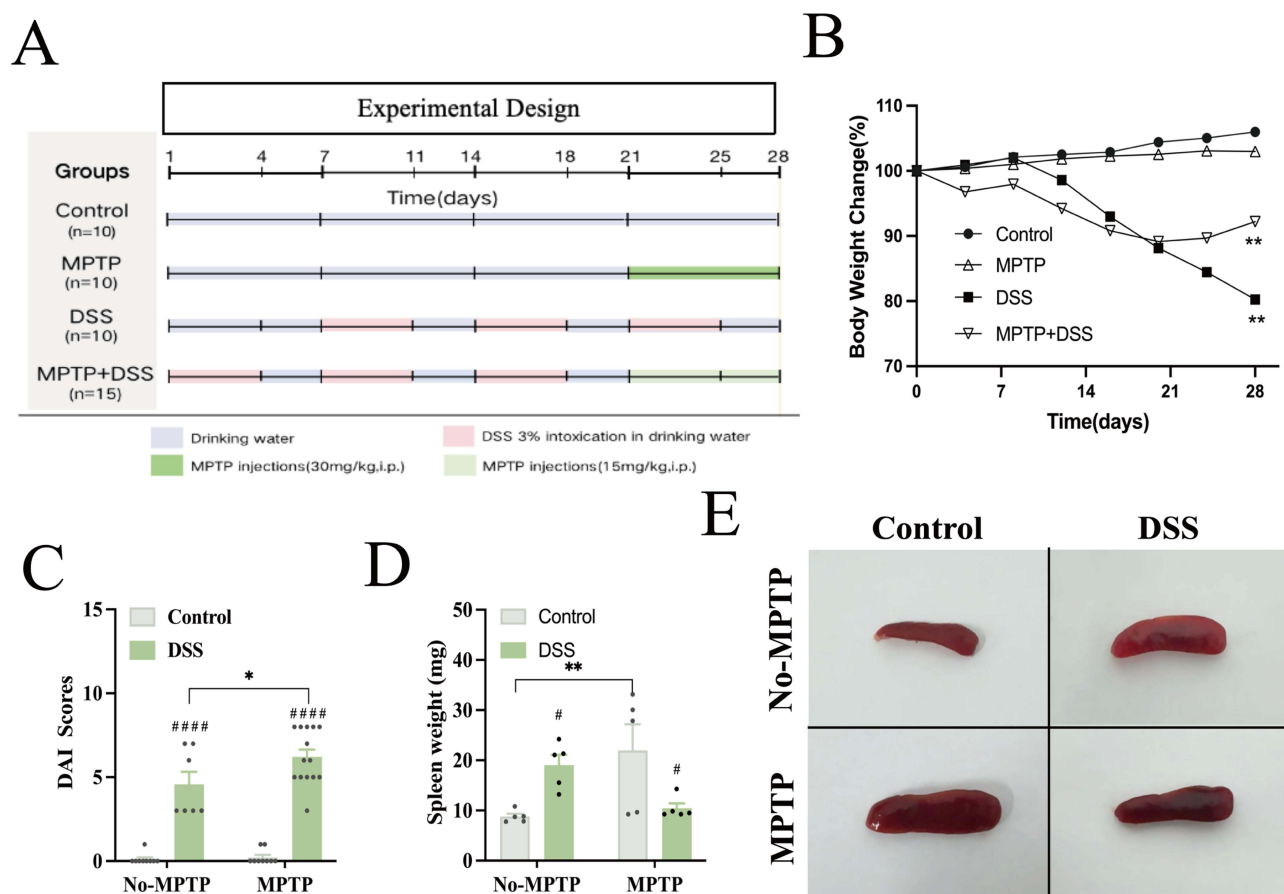


Figure 1 Characterization of mouse models. **(A)** Timeline of MPTP and DSS treatments. **(B)** Body weight change (%) during the 28-day treatment in all groups. $n=7-15$, $**p<0.01$ compared with control group. **(C)** Assessment of colitis, including body weight loss, fecal consistency and degree of blood in the stool, producing DAI scores. $n=10$. **(D)** Detailed investigation of spleen weights in each group of mice. $n=5$. **(E)** Representative images of the spleens from all experimental groups. #Intra-group comparisons, *Inter-group comparisons. * $p<0.05$, ** $p<0.01$, ##### $p<0.0001$.

We next examined whether colitis promotes or worsens the parkinsonism-associated motor features. The Rotarod test was conducted on all groups of mice, which had been trained using the same speed protocol for two days, 72 hours after the last MPTP treatment (Figure 2A).³³ As anticipated, no significant difference emerged between the control and DSS groups. However, the MPTP group showed a significantly shorter duration compared to the control group ($p<0.01$). The MPTP+DSS group also showed a significant difference compared to the DSS group ($p<0.01$) and performed worst in the Rotarod Test (Figure 2C). However, no significant difference was observed between the MPTP and DSS+MPTP groups, although the DSS+MPTP group exhibited slightly worse performance.

In the open field test (Figure 2B), the results showed that both the MPTP and DSS groups exhibited decreased distance moved in the central area ($p<0.05$). Additionally, the MPTP group demonstrated a decrease in the time spent in the center region ($p<0.05$) (Figure 2D–E). Compared to the MPTP group, the DSS+MPTP group showed a trend towards worse performance in both distance and time in center zone without statistical significance. Behavioral analysis revealed that the DSS-induced colitis did not promote an obvious motor disorder but slightly worsened the motor features induced by MPTP.

MPTP-Induced PD Mice Exhibited a Compromised Intestinal Barrier and an Exacerbated Inflammation Response in DSS-Induced Colitis

To further investigate the pathological changes in the colon of mice in each model group, H&E staining was performed on colon samples. Histological score analysis revealed that the control group exhibited normal colon characteristics, with

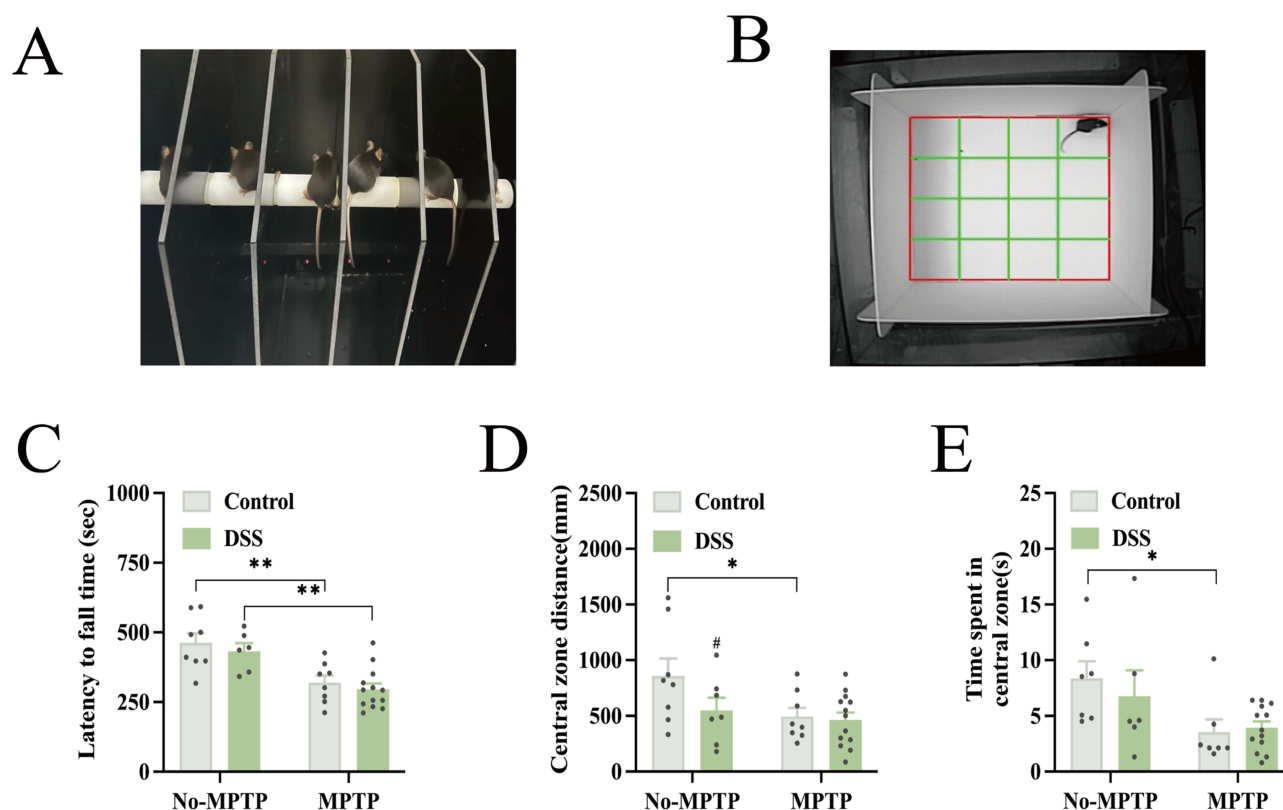


Figure 2 Behavioral tests in mice models. **(A)** Setup and test picture of the Rotarod Test. **(B)** Setup and test picture of the Open Field Test. **(C)** Results of mice maintained on the rotating rod in the Rotarod Test. n=6-13. **(D)** Total distance traveled in the center zone during the Open Field Test. n=7-13. **(E)** Total time spent in the central zone. n=6-13. #Intra-group comparisons, *Inter-group comparisons. *#p<0.05, **p<0.01.

no signs of inflammation or injury. Compared to the groups not treated with DSS, both DSS-treated groups displayed distinct pathological features associated with colitis, including crypt cell loss, increased intercrypt spacing, and crypt absence. The histological scores were significantly higher in both the DSS group ($p<0.01$) and the DSS+MPTP group ($p<0.05$) compared to the non-DSS-treated groups (Figure 3A and C). Interestingly, the histological score of the MPTP group showed a slight increase compared to the control group, though this difference was not statistically significant ($p=0.1811$). This suggested that the MPTP-induced mice may undergo potential pathological changes in the intestine despite the absence of overt histological abnormalities.

It is well established that intestinal barrier integrity is maintained by two key epithelial junction proteins, ZO-1 and Occludin. Disruption of the intestinal barrier can lead to the release of inflammatory factors into the bloodstream, triggering a systemic inflammatory response that may secondarily affect the brain. To further assess intestinal barrier integrity in the different groups, we examined the expression of Occludin and ZO-1 in colonic tissues (Figure 3B). Quantitative analysis of immunohistological data showed that Occludin protein expression was significantly decreased in the MPTP group as well as the DSS and DSS+MPTP groups compared to the control group ($p<0.01$) (Figure 3D). Similarly, the expression of ZO-1 protein also markedly decreased across groups, with the most pronounced reduction in the DSS group ($p<0.0001$) (Figure 3E). The decreased expression of ZO-1 and Occludin across groups indicated the disruption of the integrity of the intestinal barrier. Notably, even without obvious pathological changes, the MPTP-induced PD group exhibited reduced expression of junction proteins, suggesting compromised intestinal barrier function and increased colon permeability in PD mice, which were potentially regulated by LRRK2.

A previous study reported that LRRK2 expression was increased in ulcerative colitis (UC) patients.³⁴ Considering the critical regulatory role of LRRK2 in inflammatory responses in the colon, we examined the expression of LRRK2 and other inflammatory factors in the colons of mice across different groups. As expected, LRRK2 protein expression was significantly increased in the DSS-treated groups ($P<0.05$), which was consistent with previous findings. Additionally, an

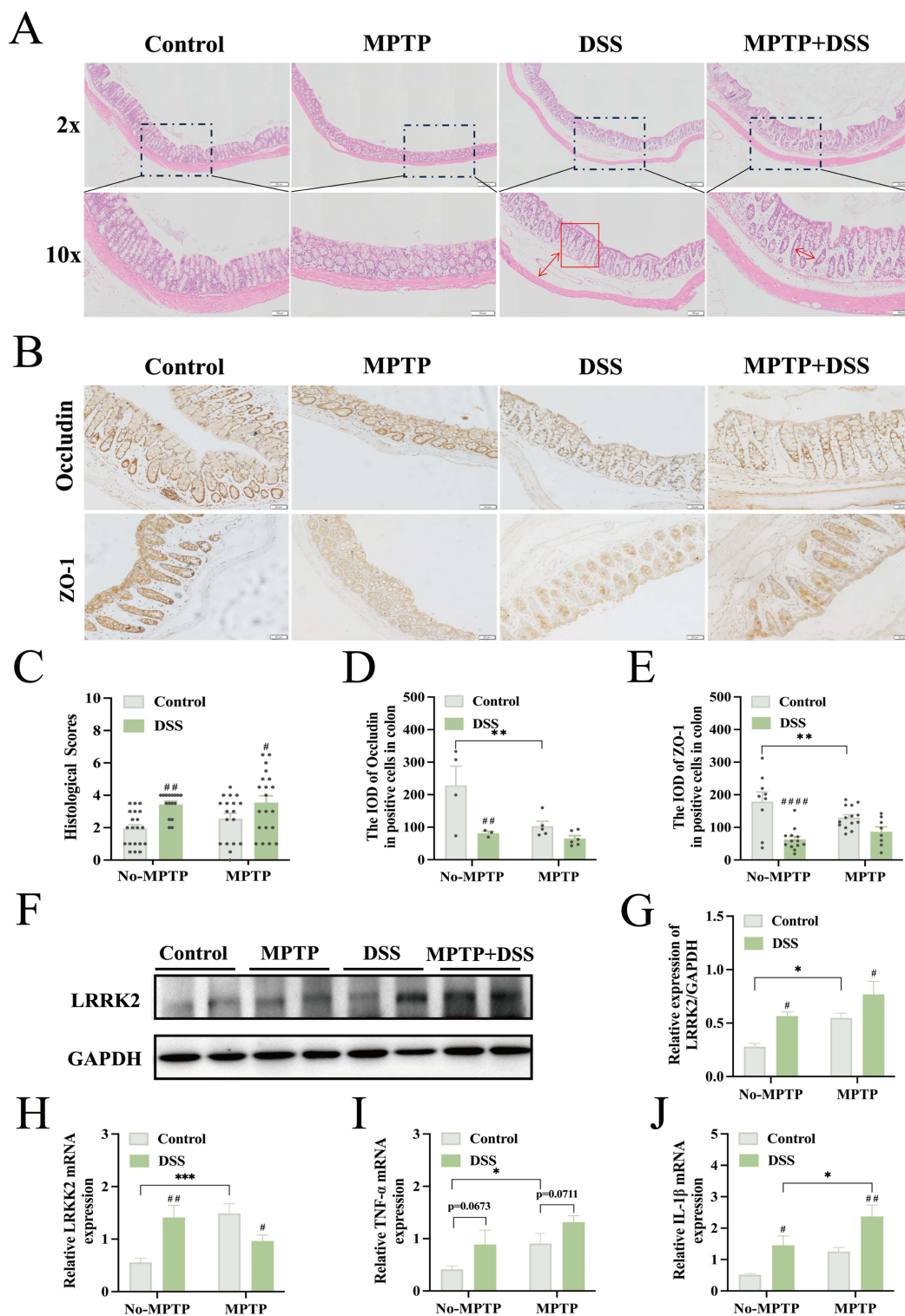


Figure 3 Intestinal barrier damage and changes in LRRK2 levels were induced by MPTP and DSS infection. **(A)** Representative histological HE sections of the colon (scale bar, 100 or 200 μ m). Red arrows indicate major pathologic changes. **(B)** Representative images of ZO-1 and Occludin in the colon (scale bar, 50 μ m, 20 \times) from four groups. **(C)** Histological colitis score, reflecting colonic inflammation severity, are shown. Black dots represent individual scores from HE-stained colon sections. (n=3 animals per group). **(D)** Quantitative analysis of immunohistochemical data for Occludin expression, black dots represent individual IOD measurements from colon sections. (n=3 animals per group). **(E)** Quantitative analysis of immunohistochemical data for ZO-1 expression, black dots represent individual IOD measurements from colon sections. (n=3 animals per group). **(F)** Western blotting showing protein level of LRRK2 in the colon, with GAPDH serving as the internal reference. **(G)** Quantification of the relative expression level of LRRK2. **(H)** The mRNA expression level of LRRK2 measured by RT-qPCR. n=4-7. **(I)** The mRNA level of TNF- α . n=6-11. **(J)** The mRNA level of IL-1 β . n=5-11. # Intra-group comparisons, *Inter-group comparisons. ##p<0.05, ###p<0.01, ****p<0.001, *****p<0.0001.

increase in LRRK2 expression was also observed in the MPTP group compared to the control group ($P < 0.05$) (Figure 3F and G). Notably, the highest expression of LRRK2 was found in the DSS+MPTP group, suggesting that MPTP treatment may further enhance LRRK2 expression in DSS-induced colitis. The analysis of LRRK2 mRNA levels showed a similar trend (Figure 3H). Additionally, we examined the mRNA levels of pro-inflammatory factors, including TNF- α and IL- β (Figure 3I and J). Interestingly, the expression patterns of TNF- α and IL- β across the groups mirrored that of LRRK2. Specifically, TNF- α expression was significantly higher in the MPTP group compared to the control group ($p < 0.05$), while IL-1 β expression was significantly elevated in the DSS-treated groups ($p < 0.05$). Moreover, IL-1 β expression was further increased in the DSS+MPTP group compared to the DSS group ($p < 0.05$). Collectively, these findings indicated that LRRK2 expression is elevated in the colon of both MPTP and DSS-treated mice and that DSS further augments LRRK2 expression in the colons of PD mice. Furthermore, the increasing levels of LRRK2 in colon tissues across the model groups were accompanied by elevated TNF- α and IL- β expression, suggesting that LRRK2 plays a role in regulating inflammation response. These findings were consistent with the observed increase in spleen size across the model groups (Figure 1D and E).

DSS-Induced Colitis May Aggravate Intracerebral Inflammation in PD Mice by Activating NF- κ B and Inhibiting Nrf2

Many previous studies have demonstrated the crosstalk between intestinal inflammation and PD neuropathology. To further explore this crosstalk, we investigated neuronal cell death and the inflammatory response in substantia nigra pars compacta (SNpc) and striatum following MPTP and DSS treatment. First, we assessed neuronal integrity by labeling Nissl bodies in the SNpc and striatum. As expected, the number of Nissl bodies in the MPTP-treated groups was significantly reduced compared to the control group, while DSS-induced colitis alone did not lead to a noticeable reduction in Nissl bodies (Figure 4A–C). Notably, in the MPTP+DSS group, the number of Nissl bodies was significantly lower than in the MPTP groups in both the SNpc and striatum. These results suggested that DSS-induced colitis may exacerbate neuronal cell loss in MPTP-induced PD mice. To further evaluate dopaminergic neuron loss, we examined the integrity of tyrosine hydroxylase (TH)-positive cells in the SNpc (Figure 4H–I). The number of TH-positive cells was significantly decreased in the MPTP-treated groups compared to other groups. Consistent with the Nissl staining results, DSS-induced colitis further exacerbated dopaminergic neuron cell loss in MPTP-induced PD mice.

Since microglial activation plays a crucial role in neuroinflammation, we next assessed Iba-1 expression, a widely used microglia marker, to determine whether DSS-induced colitis could enhance the inflammatory response in MPTP-induced PD mice (Figure 4D–G). Immunohistochemistry and Western blot analysis of the striatum revealed a significant increase in Iba-1 expression in the MPTP-treated groups compared to the control group ($p < 0.01$). Moreover, the MPTP+DSS group exhibited a significant higher level of Iba-1 expression than the MPTP group alone ($p < 0.01$) (Figure 4E and G). These findings aligned with our Nissl staining and TH-positive cells analyses, further demonstrating that colitis may exacerbate neuroinflammation in MPTP-induced PD mice.

To further characterize the inflammation in the striatum, we examined LRRK2 expression and key regulating pathways regulating neuroinflammation in PD. First, LRRK2 expression was assessed using Western blot and RT-qPCR analysis (Figure 5A, B and H). Consistent with its expression pattern in colon tissue (Figure 3F and G), LRRK2 levels were elevated following DSS and MPTP treatment. Notably, LRRK2 expression in the DSS+MPTP group was significantly higher than both the MPTP group and other groups. This suggested that DSS-induced colitis enhances LRRK2 expression in MPTP-induced PD mice. Previous studies have demonstrated that LRRK2 may regulate neuroinflammation in PD via the NF- κ B pathway, which responds to various stimuli and triggers the release of pro-inflammatory factors into the bloodstream. To explore this further, we assessed the activation status of NF- κ B p65, along with the expression of IL-6 and TNF- α – pro-inflammatory factors regulated by NF- κ B – using Western blot and RT-qPCR (Figure 5A, C, D, I and J). As expected, the levels of phosphorylated (activated) p65 (phospho-p65) increased across groups, correlating with the upregulation of LRRK2. This activation was accompanied by a rise in IL-6 and TNF- α levels, indicating a pro-inflammatory response. We also examined IL-10, an anti-inflammatory cytokine, via Western blot

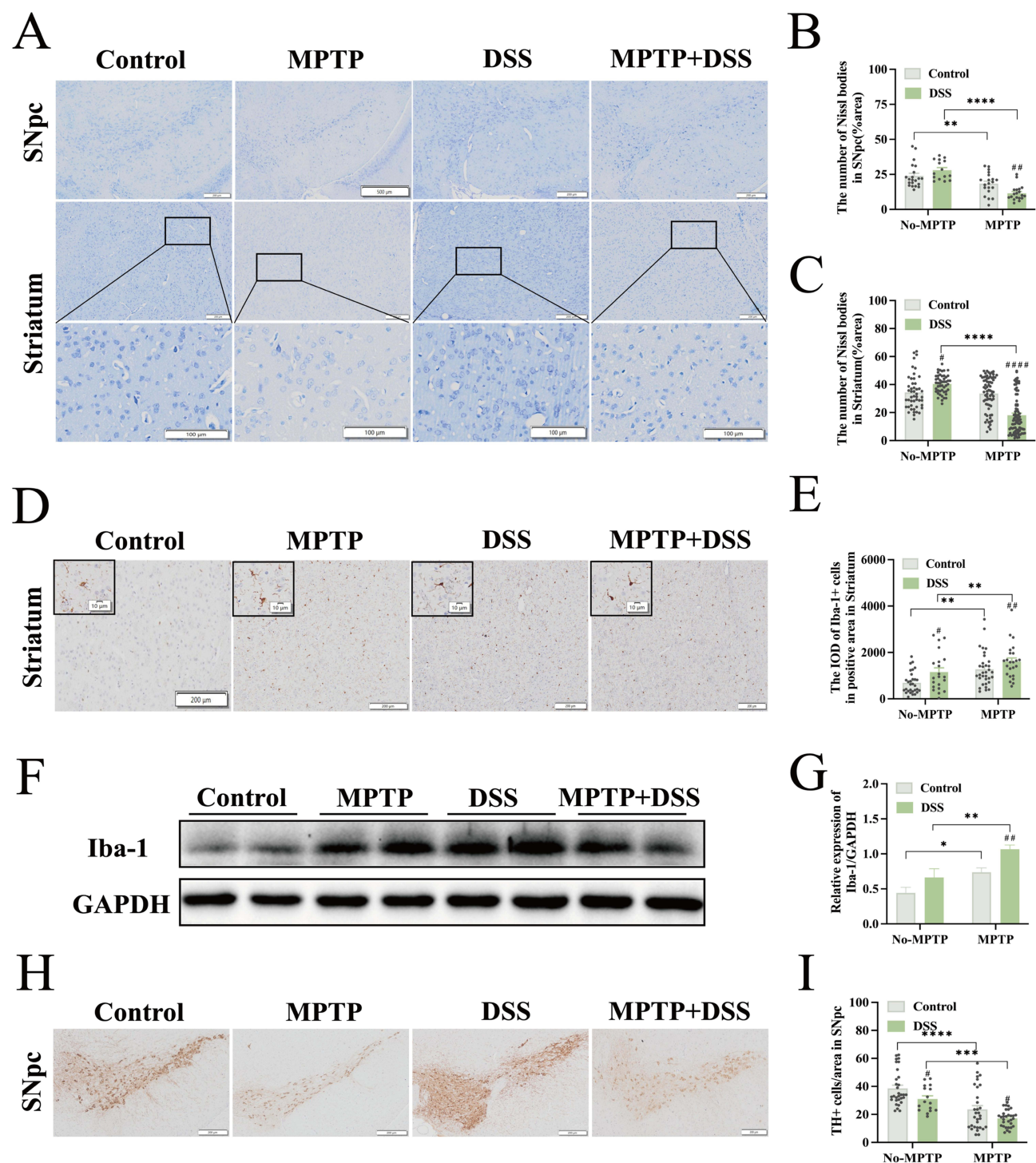


Figure 4 Neuronal cell death and inflammatory response in SNpc and Striatum following MPTP and DSS treatment. **(A)** Representative images of Nissl bodies in SNpc (scale bar 200 μm) and Striatum (scale bar above, 200 μm and scale bar below, 100 μm) from four groups. **(B)** Number of Nissl bodies per area in the SNpc. Black dots represent individual counts of Nissl bodies in SNpc sections. (n=3 animals per group). **(C)** Number of Nissl bodies per area in the Striatum. Black dots represent individual counts of Nissl bodies in Striatum sections. (n=3 animals per group). **(D)** Representative images of Iba-1-positive cells in the Striatum (scale bar, 500 μm) along with their respective local expansions (scale bar, 100 μm). **(E)** Quantitative analysis of immunohistochemical data for Iba-1 expression in the Striatum. Black dots represent individual IOD measurements from Striatum sections. (n=3 animals per group). **(F and G)** Expression level of Iba-1 protein in the Striatum. n=3-6. **(H)** Representative images of TH-positive cells in the SNpc (scale bar, 200 μm). **(I)** Quantitative analysis of TH-positive dopaminergic neurons in the SNpc. Black dots represent the number of individual TH-positive dopaminergic cells from SNpc sections. (n=3 animals per group) #Intra-group comparisons, *Inter-group comparisons. #p<0.05, ###p<0.01, ****p<0.0001.

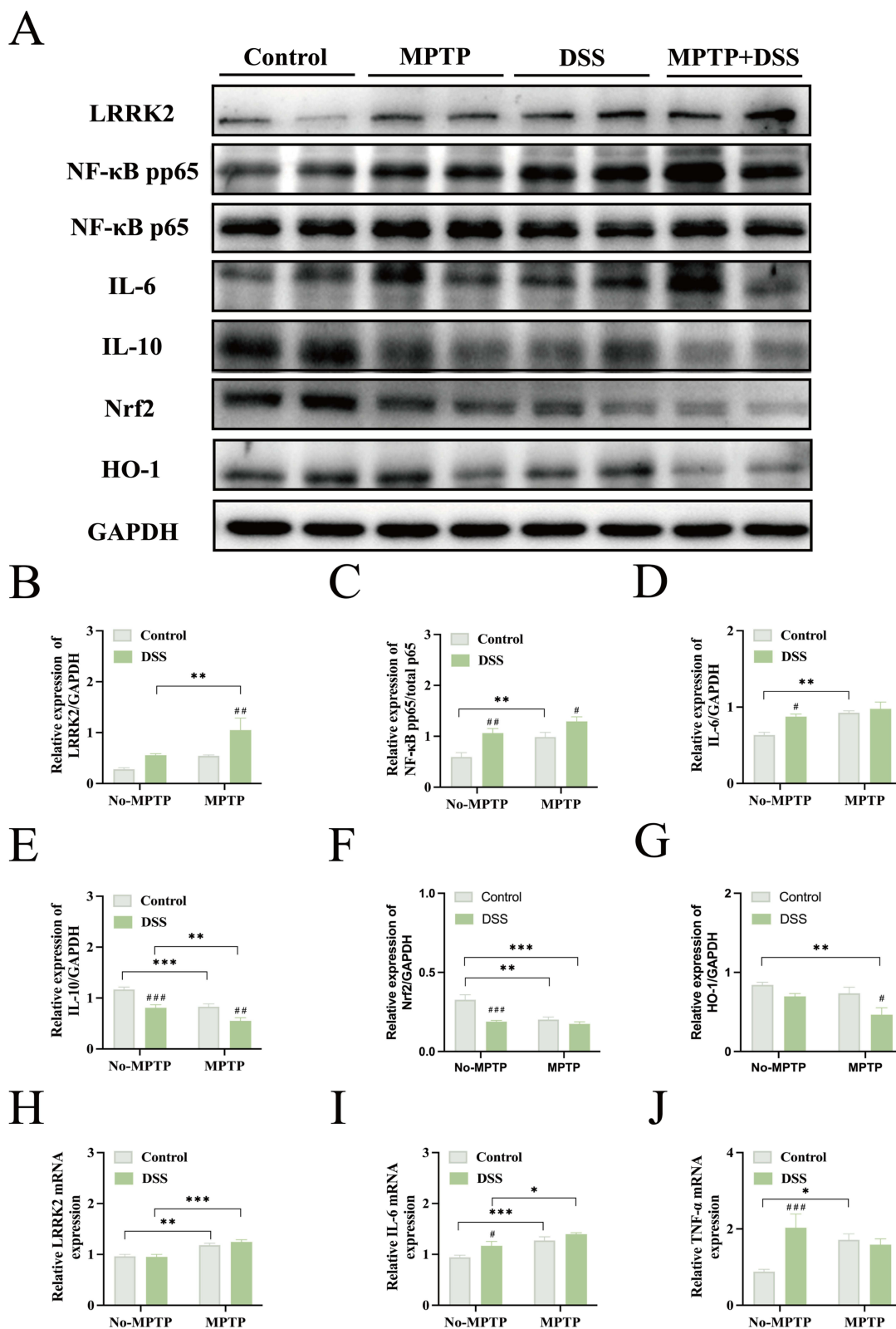


Figure 5 Activation of the NF-κB pathway and inhibition of the Nrf2 pathway in the striatum following increased LRRK2 levels. **(A)** Western blot images. $n=8$. **(B)** Quantification of the relative expression levels of LRRK2. $n=5$. **(C)** Quantification of the relative expression levels of NF-κB pp65. Total p65 served as the reference. $n=5$. **(D)** Quantification of the relative expression levels of IL-6. $n=3-5$. **(E)** Quantification of the relative expression levels of IL-10. $n=5$. **(F)** Quantification of the relative expression levels of Nrf2. $n=5$. **(G)** Quantification of the relative expression levels of HO-1. $n=6$. **(H)** mRNA level of LRRK2. $n=5$. **(I)** mRNA level of IL-6. $n=8$. **(J)** mRNA level of TNF- α . $n=7$. ###Intra-group comparisons, *Inter-group comparisons. * $p<0.05$, ** $p<0.01$, *** $p<0.001$, #### $p<0.0001$.

(Figure 5A and E). As anticipated, IL-10 expression was significantly reduced across groups, suggesting that DSS-induced colitis further suppresses the anti-inflammatory response in MPTP-induced PD mice.

Both NF- κ B and Nrf2 are key regulators of inflammation, and crosstalk between these pathways has been reported.³⁵ Our results showed that increased NF- κ B phospho-p65 activation coincided with elevated LRRK2 expression across groups. To assess Nrf2 pathway activity, we analyzed Nrf2 expression using Western blot (Figure 5A and F). Interestingly, Nrf2 expression was markedly suppressed in the striatum following MPTP and DSS treatment compared to the control group. We further evaluated Nrf2 activity by measuring expression of HO-1 (Figure 5A and G), its downstream target. HO-1 levels were reduced in response to Nrf2 inhibition, reinforcing the suppression of the Nrf2 pathway.

Taken together, these findings suggest that DSS-induced colitis may exacerbate neuroinflammation in PD mice by activating NF- κ B and inhibiting Nrf2. Moreover, LRRK2 may serve as a potential regulator mediating the crosstalk between NF- κ B and Nrf2 in PD.

Discussion

In this study, we constructed DSS+MPTP-induced dual-hit, DSS-induced colitis, and MPTP-induced PD mouse models. Through investigating LRRK2 expression levels, the activity of NF- κ B and Nrf2 pathways – both known to regulate inflammation in the colon and brain – as well as key inflammatory factors (TNF- α , IL-1 β , IL-6 and IL-10), we found that LRRK2 expression was markedly increased in both the colon and brain in the dual-hit group compared to other groups. In the colon, increased LRRK2 expression was accompanied by a reduction in key junction proteins and an increase in inflammatory factors. In the SNpc and striatum, elevated LRRK2 expression was associated with NF- κ B p65 activation and Nrf2 inhibition. Moreover, these changes were more pronounced in the dual-hit model. These results suggest that MPTP-induced PD may compromise intestinal barrier function in the colon, while DSS-induced colitis may trigger an inflammatory response in the brain. Our findings expand the current understanding of the crosstalk between intestinal inflammation and PD neuropathology.

It has been demonstrated that LRRK2 protein increases intestinal permeability, facilitating the translocation of the bacterial metabolite lipopolysaccharide (LPS) from the gut microbiota into the bloodstream. This leads to elevated circulating LPS levels, further contributing to inflammation.³⁶ In a seminal experiment, Alessia et al intraperitoneal injected mice with MPTP and subsequently analyzed colon samples across a concentration gradient. The results showed that MPTP treatment led to increased expression of phosphorylated LRRK2 (Ser935) and more severe colonic inflammation compared to the control group.³⁷ Consistent with previous studies, our study also demonstrated that intestinal inflammation compromises intestinal barrier function. Specifically, we observed that both MPTP and DSS treatments significantly reduced the expression of key colonic tight junction proteins, including ZO-1 and Occludin, which were potentially regulated by LRRK2. (Figure 3). This finding aligns with a previous human study, which reported increased intestinal permeability in both PD and CD patients, particularly in the latter. Additionally, the study was found that Claudin-2 was highly upregulated in inflamed epithelium, while ZO-1 and Occludin were significantly reduced.³⁸

In the present study, both MPTP and DSS treatments increased intestinal LRRK2 expression in the colon. Furthermore, the colon of dual-hit (MPTP+DSS) mice exhibited an even more pronounced increase in LRRK2 protein levels (Figure 3). This was accompanied by elevated inflammatory factors, including TNF- α and IL-1 β . Gardet et al previously reported that LRRK2 kinase is highly expressed in inflamed intestinal tissues and plays a role in bacterial phagocytosis during macrophage infection.³⁹ Another study demonstrated that LRRK2 phosphorylation increases in inflamed colonic mucosa following acute colitis, with IFN- γ production suggesting an IFN- γ -dependent regulatory mechanism.⁴⁰ Additionally, deficient reactive oxygen species (ROS) production has been linked to severe chronic DSS-induced colitis in Ncf1/p47phox-mutant mice.⁴¹ Like our observations in the colon, LRRK2 expression levels were also elevated in the brain across all model groups. Notably, DSS treatment further exacerbated LRRK2 protein levels in the brain of MPTP+DSS mice (Figure 4). In this study, Sharma et al found that DSS-mediated colitis mice develop degeneration of dopaminergic neurons TH and activation of astrocyte GFAP in the SNpc and striatum, which worsens neurodegeneration in the brain when mice are exposed to Rotenone.⁴² Lin et al found that mild chronic colitis promotes LRRK2 expression via activation of the TNF- α pathway in G2019S mice with Parkinson's disease characteristics. Furthermore, treatment with an anti-TNF- α monoclonal antibody reduced intestinal inflammation, suppressed microglial

activation, and alleviated neuronal degeneration.²⁴ In their study, LRRK2 G2019S colitis mice exhibited a significant decline in TH-positive cells compared to other groups, which aligns with our findings—MPTP+DSS mice showed a significant reduction in TH-positive cells compared to the MPTP-only group. Additionally, a similar modeling approach used by Martinez et al revealed that striatal Iba-1 expression levels in MPTP+DSS mice showed an increasing trend compared to the MPTP group, which is consistent with the results of our study.⁴³

LRRK2 kinase activity has been identified as a marker of neuronal function and toxicity.⁴⁴ However, it is noteworthy that polymorphisms linked to an increased risk of developing PD and IBD have been identified in the coding and non-coding regions of the LRRK2 gene. These polymorphisms are not confined to the kinase structural domain. As a result, LRRK2 kinase activity may be enhanced even without mutations or polymorphisms in an inflammatory environment, leading to the production of pro-inflammatory cytokines and increased NF- κ B activity.⁴⁵ Supporting this notion, studies have shown that transfecting HEK293 cells with a WT LRRK2 plasmid leads to NF- κ B pathway activation compared to a control plasmid.³⁹ Additionally, Russo et al demonstrated that LRRK2 can modulate the cAMP-PKA-NF- κ B p50 pathway to facilitate bacterial metabolite (LPS) production and promote α -syn aggregation.⁴⁶ In contrast, subsequent studies have reported that LRRK2 KO mice exhibit essentially unchanged NF- κ B component (including p65) production in response to LPS stimulation.²² Similarly, Hongge et al found that IL-1 β stimulation of human vascular endothelial cells (HUVECs) resulted in increased nuclear p65 expression and NF- κ B activation when the cells were transfected with an LRRK2-expressing plasmid.⁴⁷ The NF- κ B signaling pathway plays a key role in activating microglia in the brain, which in turn triggers the transcription of inflammation-associated genes and induces a central inflammatory response.⁴⁸ Once activated, microglia—innate immune cells of the brain—release large quantities of inflammatory factors, promoting oxidative stress and initiating neuroinflammatory mechanisms.⁴⁹ In the present study, we demonstrated that upregulation of LRRK2 protein expression activated the NF- κ B pathway, leading to a significant increase in the downstream inflammatory factor IL-6 (Figure 5). IL-6 is particularly noteworthy, as it plays a pivotal role in linking local inflammation to a systemic inflammatory response. Given the increased spleen mass observed in all model groups, we hypothesize that MPTP and DSS treatments contribute to a systemic inflammatory response (Figure 5). Nuclear factor erythroid 2-related factor (Nrf2) is a transcription factor that protects cells from oxidative stress by inducing the expression of antioxidant genes.⁵⁰ Kawakami et al analyzed brain tissues from LRRK2 transgenic mice and SH-SY5Y cells overexpressing LRRK2, revealing that Nrf2 expression—as well as its downstream antioxidant targets, including HO-1 and GPX—was reduced at both the protein and mRNA levels. Furthermore, knocking down glycogen synthase kinase-3 β (GSK-3 β) restored Nrf2 expression in SH-SY5Y cells overexpressing LRRK2, suggesting a regulatory interaction between GSK-3 β and Nrf2.⁵¹ In our study, we similarly observed that both MPTP and DSS treatments reduced Nrf2 and HO-1 expression in mouse brains, with the MPTP+DSS group exhibiting the most significant decrease in HO-1 protein levels (Figure 5). These findings are consistent with previous studies. Additionally, Skibinski et al demonstrated that Nrf2 overexpression could mitigate LRRK2- and α -syn-induced neuronal toxicity, further highlighting the protective role of Nrf2 in neurodegenerative processes.⁵²

Indeed, Nrf2 and NF- κ B are key pathways that regulate the body's response to oxidative stress and inflammation, maintaining a delicate balance.^{53–55} Many previous studies have demonstrated that NF- κ B can regulate Nrf2 activity and influence the expression of its downstream target genes. Conversely, Nrf2 deficiency leads to increased NF- κ B expression, followed by elevated production of inflammatory factors. However, the molecular mechanisms underlying the cross-talk between Nrf2 and NF- κ B remain largely unknown. The present study found that elevated LRRK2 expression was associated with NF- κ B activation and Nrf2 inhibition. Thus, we propose that LRRK2 may be a potential regulator mediating the interplay between NF- κ B and Nrf2 in PD.

Conclusions

In conclusion, our findings demonstrate that mild chronic colitis induced by DSS may exacerbate brain inflammation in MPTP-induced PD mice by upregulating LRRK2 expression, leading to NF- κ B activation and Nrf2 inhibition. We suggest that LRRK2 may play a role in regulating the NF- κ B/Nrf2 interplay in PD. However, the precise regulatory mechanisms require further investigation through future studies.

Acknowledgments

This work was supported by the National Natural Science Foundation of China (81971196). We would like to thank the Analytical & Testing Center of Wuhan University of Science and Technology for the help with in vivo imaging of mice analysis.

Disclosure

The authors declare no conflicts of interest regarding the present work.

References

1. Dorsey ER, Bloem BR. The Parkinson Pandemic-A call to action. *JAMA Neurol.* **2018**;75(1):9–10. doi:10.1001/jamaneurol.2017.3299
2. Morris HR, Spillantini MG, Sue CM, Williams-Gray CH. The pathogenesis of Parkinson's disease. *Lancet.* **2024**;403(10423):293–304. doi:10.1016/S0140-6736(23)01478-2
3. Galiano-Landeira J, Torra A, Vila M, Bove J. CD8 T cell nigral infiltration precedes synucleinopathy in early stages of Parkinson's disease. *Brain.* **2020**;143(12):3717–3733. doi:10.1093/brain/awaa269
4. Mills KHG. IL-17 and IL-17-producing cells in protection versus pathology. *Nat Rev Immunol.* **2023**;23(1):38–54. doi:10.1038/s41577-022-00746-9
5. Wang W, Nguyen LT, Burlak C, et al. Caspase-1 causes truncation and aggregation of the Parkinson's disease-associated protein alpha-synuclein. *Proc Natl Acad Sci U S A.* **2016**;113(34):9587–9592. doi:10.1073/pnas.1610099113
6. Fasano A, Visanji NP, Liu LW, Lang AE, Pfeiffer RF. Gastrointestinal dysfunction in Parkinson's disease. *Lancet Neurol.* **2015**;14(6):625–639. doi:10.1016/S1474-4422(15)00007-1
7. Leta V, Klingelhoefer L, Longardner K, et al. Gastrointestinal barriers to levodopa transport and absorption in Parkinson's disease. *Eur J Neurol.* **2023**;30(5):1465–1480. doi:10.1111/ene.15734
8. Li Y, Chen Y, Jiang L, et al. Intestinal inflammation and Parkinson's disease. *Aging Dis.* **2021**;12(8):2052–2068. doi:10.14336/AD.2021.0418
9. Peter I, Dubinsky M, Bressman S, et al. Anti-tumor necrosis factor therapy and incidence of Parkinson disease among patients with inflammatory bowel disease. *JAMA Neurol.* **2018**;75(8):939–946. doi:10.1001/jamaneurol.2018.0605
10. Wallen ZD, Demirkan A, Twa G, et al. Metagenomics of Parkinson's disease implicates the gut microbiome in multiple disease mechanisms. *Nat Commun.* **2022**;13(1):6958. doi:10.1038/s41467-022-34667-x
11. Keshavarzian A, Engen P, Bonvegna S, Cilia R. The gut microbiome in Parkinson's disease: a culprit or a bystander? *Prog Brain Res.* **2020**;252:357–450. doi:10.1016/bs.pbr.2020.01.004
12. Houser MC, Tansey MG. The gut-brain axis: is intestinal inflammation a silent driver of Parkinson's disease pathogenesis? *NPJ Parkinsons Dis.* **2017**;3:3. doi:10.1038/s41531-016-0002-0
13. Hou YF, Shan C, Zhuang SY, et al. Gut microbiota-derived propionate mediates the neuroprotective effect of osteocalcin in a mouse model of Parkinson's disease. *Microbiome.* **2021**;9(1):34. doi:10.1186/s40168-020-00988-6
14. Dodiya HB, Forsyth CB, Voigt RM, et al. Chronic stress-induced gut dysfunction exacerbates Parkinson's disease phenotype and pathology in a rotenone-induced mouse model of Parkinson's disease. *Neurobiol Dis.* **2020**;135:104352. doi:10.1016/j.nbd.2018.12.012
15. Grigoletto J, Miraglia F, Benvenuti L, et al. Velusetrag rescues GI dysfunction, gut inflammation and dysbiosis in a mouse model of Parkinson's disease. *NPJ Parkinsons Dis.* **2023**;9(1):140. doi:10.1038/s41531-023-00582-1
16. Chakrabarti A, Geurts L, Hoyles L, et al. The microbiota-gut-brain axis: pathways to better brain health. Perspectives on what we know, what we need to investigate and how to put knowledge into practice. *Cell Mol Life Sci.* **2022**;79(2):80. doi:10.1007/s00018-021-04060-w
17. Kars ME, Wu Y, Stenson PD, et al. The landscape of rare genetic variation associated with inflammatory bowel disease and Parkinson's disease comorbidity. *Genome Med.* **2024**;16(1):66. doi:10.1186/s13073-024-01335-2
18. Russo I, Bubacco L, Greggio E. LRRK2 as a target for modulating immune system responses. *Neurobiol Dis.* **2022**;169:105724. doi:10.1016/j.nbd.2022.105724
19. Zheng Z, Zhang S, Liu X, et al. LRRK2 regulates ferroptosis through the system Xc-GSH-GPX4 pathway in the neuroinflammatory mechanism of Parkinson's disease. *J Cell Physiol.* **2024**;239(5):e31250. doi:10.1002/jcp.31250
20. Feng YK, Wu QL, Peng YW, et al. Oral P. gingivalis impairs gut permeability and mediates immune responses associated with neurodegeneration in LRRK2 R1441G mice. *J Neuroinflammation.* **2020**;17(1):347. doi:10.1186/s12974-020-02027-5
21. Moehle MS, Webber PJ, Tse T, et al. LRRK2 inhibition attenuates microglial inflammatory responses. *J Neurosci.* **2012**;32(5):1602–1611. doi:10.1523/JNEUROSCI.5601-11.2012
22. Cabezaudo D, Tsafaras G, Van Acker E, Van den Haute C, Baekelandt V. Mutant LRRK2 exacerbates immune response and neurodegeneration in a chronic model of experimental colitis. *Acta Neuropathol.* **2023**;146(2):245–261. doi:10.1007/s00401-023-02595-9
23. Liu Z, Lenardo MJ. The role of LRRK2 in inflammatory bowel disease. *Cell Res.* **2012**;22(7):1092–1094. doi:10.1038/cr.2012.42
24. Lin CH, Lin HY, Ho EP, et al. Mild chronic colitis triggers Parkinsonism in LRRK2 mutant mice through activating TNF-alpha pathway. *Mov Disord.* **2022**;37(4):745–757. doi:10.1002/mds.28890
25. Takagawa T, Kitani A, Fuss I, et al. An increase in LRRK2 suppresses autophagy and enhances Dectin-1-induced immunity in a mouse model of colitis. *Sci Transl Med.* **2018**;10(444). doi:10.1126/scitranslmed.aan8162
26. Lin CH, Lin HI, Chen ML, et al. Lovastatin protects neurite degeneration in LRRK2-G2019S parkinsonism through activating the Akt/Nrf pathway and inhibiting GSK3beta activity. *Hum Mol Genet.* **2016**;25(10):1965–1978. doi:10.1093/hmg/ddw068
27. Mustapha M, Mat Taib CN. MPTP-induced mouse model of Parkinson's disease: a promising direction of therapeutic strategies. *Bosn J Basic Med Sci.* **2021**;21(4):422–433. doi:10.17305/bjbm.2020.5181
28. Zhang QS, Heng Y, Mou Z, Huang JY, Yuan YH, Chen NH. Reassessment of subacute MPTP-treated mice as animal model of Parkinson's disease. *Acta Pharmacol Sin.* **2017**;38(10):1317–1328. doi:10.1038/aps.2017.49
29. Gil-Martinez AL, Cuenca-Bermejo L, Gonzalez-Cuello AM, et al. Identification of differentially expressed genes profiles in a combined mouse model of Parkinsonism and colitis. *Sci Rep.* **2020**;10(1):13147. doi:10.1038/s41598-020-69695-4

30. Dong L, Xie J, Wang Y, et al. Mannose ameliorates experimental colitis by protecting intestinal barrier integrity. *Nat Commun.* 2022;13(1):4804. doi:10.1038/s41467-022-32505-8
31. Liu W, Zhang Y, Qiu B, et al. Quinoa whole grain diet compromises the changes of gut microbiota and colonic colitis induced by dextran Sulfate sodium in C57BL/6 mice. *Sci Rep.* 2018;8(1):14916. doi:10.1038/s41598-018-33092-9
32. Chassaing B, Srinivasan G, Delgado MA, Young AN, Gewirtz AT, Vijay-Kumar M. Fecal lipocalin 2, a sensitive and broadly dynamic non-invasive biomarker for intestinal inflammation. *PLoS One.* 2012;7(9):e44328. doi:10.1371/journal.pone.0044328
33. Melo-Thomas L, Gil-Martinez AL, Cuenca L, et al. Electrical stimulation or MK-801 in the inferior colliculus improve motor deficits in MPTP-treated mice. *Neurotoxicology.* 2018;65:38–43. doi:10.1016/j.neuro.2018.01.004
34. Yan J, Yu W, Wang G, et al. LRRK2 deficiency mitigates colitis progression by favoring resolution of inflammation and restoring homeostasis of gut microbiota. *Genomics.* 2022;114(6):110527. doi:10.1016/j.ygeno.2022.110527
35. Bhandari R, Khanna G, Kaushik D, Kuhad A. Divulging the intricacies of crosstalk between NF-Kb and Nrf2-Keap1 pathway in neurological complications of COVID-19. *Mol Neurobiol.* 2021;58(7):3347–3361. doi:10.1007/s12035-021-02344-7
36. Shi H, Yu Y, Lin D, et al. beta-glucan attenuates cognitive impairment via the gut-brain axis in diet-induced obese mice. *Microbiome.* 2020;8(1):143. doi:10.1186/s40168-020-00920-y
37. Filippone A, Mannino D, Cucinotta L, et al. Rebalance of mitophagy by inhibiting LRRK2 improves colon alterations in an MPTP in vivo model. *iScience.* 2024;27(10):110980. doi:10.1016/j.isci.2024.110980
38. Prasad S, Mingrino R, Kaukinen K, et al. Inflammatory processes have differential effects on claudins 2, 3 and 4 in colonic epithelial cells. *Lab Invest.* 2005;85(9):1139–1162. doi:10.1038/labinvest.3700316
39. Gardet A, Benita Y, Li C, et al. LRRK2 is involved in the IFN-gamma response and host response to pathogens. *J Immunol.* 2010;185(9):5577–5585. doi:10.4049/jimmunol.1000548
40. Liu Z, Lee J, Krummey S, et al. The kinase LRRK2 is a regulator of the transcription factor NFAT that modulates the severity of inflammatory bowel disease. *Nat Immunol.* 2011;12(11):1063–1070. doi:10.1038/ni.2113
41. Rodrigues-Sousa T, Ladeirinha AF, Santiago AR, et al. Deficient production of reactive oxygen species leads to severe chronic DSS-induced colitis in Nef1/p47phox-mutant mice. *PLoS One.* 2014;9(5):e97532. doi:10.1371/journal.pone.0097532
42. Sharma N, Sharma M, Thakkar D, et al. Chronic DSS-induced colitis exacerbates Parkinson's disease phenotype and its pathological features following intragastric rotenone exposure. *ACS Pharmacol Transl Sci.* 2025;8(2):346–367. doi:10.1021/acspstsci.4c00286
43. Gil-Martinez AL, Estrada C, Cuenca L, et al. Local gastrointestinal injury exacerbates inflammation and dopaminergic cell death in Parkinsonian mice. *Neurotox Res.* 2019;35(4):918–930. doi:10.1007/s12640-019-0010-z
44. Taymans JM, Fell M, Greenamyre T, et al. Perspective on the current state of the LRRK2 field. *NPJ Parkinsons Dis.* 2023;9(1):104. doi:10.1038/s41531-023-00544-7
45. Peter I, Strober W. Immunological features of LRRK2 function and its role in the gut-brain axis governing Parkinson's disease. *J Parkinsons Dis.* 2023;13(3):279–296. doi:10.3233/jpd-230021
46. Herrick MK, Tansey MG. Is LRRK2 the missing link between inflammatory bowel disease and Parkinson's disease? *NPJ Parkinsons Dis.* 2021;7(1):26. doi:10.1038/s41531-021-00170-1
47. Hongge L, Kexin G, Xiaojie M, et al. The role of LRRK2 in the regulation of monocyte adhesion to endothelial cells. *J Mol Neurosci.* 2015;55(1):233–239. doi:10.1007/s12031-014-0312-9
48. Rohr MW, Narasimhulu CA, Rudeski-Rohr TA, Parthasarathy S. Negative effects of a high-fat diet on intestinal permeability: a review. *Adv Nutr.* 2020;11(1):77–91. doi:10.1093/advances/nmz061
49. Wang XL, Li L. Microglia regulate neuronal circuits in homeostatic and high-fat diet-induced inflammatory conditions. *Front Cell Neurosci.* 2021;15:722028. doi:10.3389/fncel.2021.722028
50. He F, Ru X, Wen T. NRF2, a transcription factor for stress response and beyond. *Int J Mol Sci.* 2020;21(13). doi:10.3390/ijms21134777
51. Kawakami F, Imai M, Tamaki S, et al. Nrf2 expression is decreased in LRRK2 transgenic mouse brain and LRRK2 overexpressing SH-SY5Y cells. *Biol Pharm Bull.* 2023;46(1):123–127. doi:10.1248/bpb.b22-00356
52. Skibinski G, Hwang V, Ando DM, et al. Nrf2 mitigates LRRK2- and alpha-synuclein-induced neurodegeneration by modulating proteostasis. *Proc Natl Acad Sci U S A.* 2017;114(5):1165–1170. doi:10.1073/pnas.1522872114
53. Casper E. The crosstalk between Nrf2 and NF-kappaB pathways in coronary artery disease: can it be regulated by SIRT6? *Life Sci.* 2023;330:122007. doi:10.1016/j.lfs.2023.122007
54. Sivandzade F, Prasad S, Bhalerao A, Cucullo L. NRF2 and NF-kB interplay in cerebrovascular and neurodegenerative disorders: molecular mechanisms and possible therapeutic approaches. *Redox Biol.* 2019;21:101059. doi:10.1016/j.redox.2018.11.017
55. Wardyn JD, Ponsford AH, Sanderson CM. Dissecting molecular cross-talk between Nrf2 and NF-kappaB response pathways. *Biochem Soc Trans.* 2015;43(4):621–626. doi:10.1042/BST20150014